文章编号：1001－9014(2018)04－0385－04

DOI:10.11972/j.issn.1001－9014.2018.04.001

Growth optimization of GaAs-based InAs/AlSb 2DEG structure

CUI Xiao-Ran[1,2], LYU Hong-Liang[1], LI Jin-Lun[4,2], SU Xiang-Bin[5,2], XU Ying-Qiang[2,3*], NIU Zhi-Chuan[2,3]

(1. School of Microelectronics, Xidian University, Xi'an 710071, China;
2. State Key Laboratory for Superlattices, Institute of Semiconductors, Chinese Academy of Sciences, Beijing 100083, China;
3. College of Materials Science and Opto-Electronic Technology, University of Chinese Academy of Sciences, Beijing 100049, China;
4. Department of Missile Engineering, Shijiazhuang Campus, Army Engineering University, Shijiazhuang 050003, China;
5. Institute of Photonics and Photon-Technology, Northwest University, Xi'an 710069, China)

Abstract: InAs/AlSb two-dimensional electron gas (2DEG) structures were successfully grown by MBE equipment. 2DEG characteristics of samples were improved by optimizing the the thickness of AlGaSb buffer layer, the thickness of InAs/AlSb interface layer, and the thickness of AlSb spacer. The InAs/AlSb 2DEG structure sample with an electron mobility of 20500 $cm^2/V \cdot s$ and a sheet electron density of $2.0 \times 10^{12}/cm^2$ were achieved when the thickness of AlSb spacer is fixed at 5 nm. It provides a reference for the research and fabrication of InAs/AlSb HEMT.

Key words: 2DEG, mobility, high electron mobility transistor (HEMT), molecular beam epitaxy (MBE)
PACS: 71.10.Ca, 73.40.Kp, 81.05.Ea

GaAs 基 InAs/AlSb 二维电子气结构的生长优化

崔晓然[1,2], 吕红亮[1], 李金伦[4,2], 苏向斌[5,2], 徐应强[2,3], 牛智川[2,3*]

(1. 西安电子科技大学 微电子学院,陕西 西安 710071;
2. 中国科学院半导体研究所 超晶格实验室,北京 100083;
3. 中国科学院大学 材料科学与光电技术学院,北京 100049;
4. 中国人民解放军陆军工程大学石家庄校区 导弹工程系,河北 石家庄 050003;
5. 西北大学 光子学与光子技术研究所,陕西 西安 710069)

摘要:采用分子束外延设备(MBE),外延生长了InAs/AlSb二维电子气结构样品.样品制备过程中,通过优化AlGaSb缓冲层厚度和InAs/AlSb界面厚度、改变AlSb隔离层厚度,分别对比了材料二维电子气特性的变化,并在隔离层厚度为5 nm时,获得了室温电子迁移率为20500 $cm^2/V \cdot s$,面电荷密度为$2.0 \times 10^{12}/cm^2$的InAs/AlSb二维电子气结构样品,为InAs/AlSb高电子迁移率晶体管的研究和制备提供了参考依据.

关 键 词:二维电子气;迁移率;高电子迁移率晶体管(HEMT);分子束外延(MBE)

中图分类号:TN386.3　　**文献标识码**:A

Introduction

The first high electron mobility transistor (HEMT) is fabricated with GaAs channels and AlGaAs barriers in 1978[1-2]. Since then, several material systems like InAs/AlSb have been studied. The combination of InAs and AlSb leads to a staggered band lineup (type-II) as well as one of the largest conduction band discontinuities among III-V based heterostructures[3-5]. Such a deep quantum well allows excellent electron confinement, high electron concentration and enhanced radiation tolerance. There are also high values of carrier mobility, saturation velocity, and electron sheet charge density in an InAs channel[6-7]. InAs/AlSb HEMTs exhibit similar performance as the established InGaAs/InAlAs HEMT at one-

Received date: 2017-11-28, **revised date**: 2018-04-12　　**收稿日期**:2017-11-28, **修回日期**:2018-04-12
Foundation items:Supported by the National Key Technologies R&D Program (2016CBYFB0402403)
Biography:CUI Xiao-Ran (1992-), male, Shijiazhuang, China, Master. Research area involves semiconductor materials and devices. E-mail:cxr_904@164.com
* **Corresponding author**:E-mail: yingqxu@semi.ac.cn

fourth of its power dissipation. All these advantages make InAs/AlSb material system a promising candidate to apply in high-speed devices and low-power circuits[8-10].

However, due to lack of zinc blende insulating substrates with lattice constant matched to InAs, S. I. GaAs substrates are used for the growth of InAs/AlSb HEMTs widely, which causes 7% lattice mismatch between an InAs channel and a GaAs substrate.

In this study, InAs/AlSb 2DEG structures are grown on S. I. GaAs (100) substrates by MBE. The growth parameters are optimized by series of experiments to achieve better performance.

1 Experiments

In this study, all samples were grown on S. I. GaAs (100) substrates. The growth temperature represented thermocouple temperature. To monitor deoxidization, *in-situ* reflection high energy electron diffraction (RHEED) was used. AFM was used to measure surface morphology in contact mode. Electron mobility and sheet electron density were measured by Van der Pauw measurement.

The structure of InAs/AlSb 2DEG was shown in Fig. 1. After oxide desorption process, GaAs buffer was deposited. Then AlSb and AlGaSb buffer layer were grown. On the buffer layer, AlSb/InAs/AlSb sandwich structure was deposited. Due to the amphoteric behavior of silicon in III-V compounds[11], there was an InAs layer for Si doping. InAlAs etch stopper and InAs capper were grown subsequently.

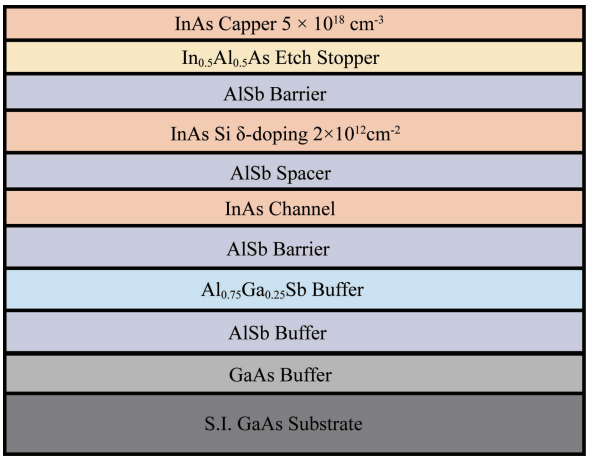

Fig. 1 Structure of InAs/AlSb 2DEG
图 1 InAs/AlSb 二维电子气结构

2 Results and discussions

2.1 Thickness of AlGaSb buffer layer

Since the thickness of AlGaSb buffer layer has an influence on surface morphology, samples (a-f) were grown at different AlGaSb buffer thickness (100 nm, 250 nm, 500 nm, 750 nm, 1 μm, and 1.5 μm). As shown in Fig. 2, after deoxidization and 200 nm GaAs buffer layer depositing, AlSb buffer and different thicknesses of $Al_{0.75}Ga_{0.25}Sb$ buffer were grown on S. I. GaAs substrate at growth rate of 0.67 ML/s. Then a 5 nm GaSb layer was deposited on $Al_{0.75}Ga_{0.25}Sb$ buffer layer to prevent oxidation.

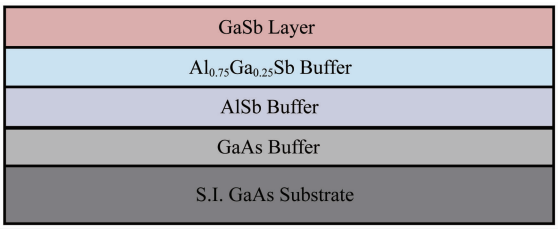

Fig. 2 Schematic diagram of GaAs/AlSb/AlGaSb/GaSb buffer layer
图 2 GaAs/AlSb/AlGaSb/GaSb 缓冲层示意图

The surface morphologies of a series of samples are shown in Fig. 3. From these images, there are pyramidal mounds on the surface of AlGaSb layers. These mounds are formed by monolayer spiral steps centered around screw dislocations originated from the interface between the AlSb and GaAs[12]. Such kind of images can also be seen on the surface of InAs or GaSb epitaxy on Si substrates[13-20]. These abreast mounds show rectangle bases. With AlGaSb thickness increasing, heights of the mounds get lower and fissures resulted from the boundary of neighboring mounds coalesce. The RMS values of the samples are shown in Fig. 4. From Fig. 4, we can see that sample (e) is the smoothest one. It can also be found that from 100 nm to 1.5 μm, the RMS values decrease and the surface gets smoother.

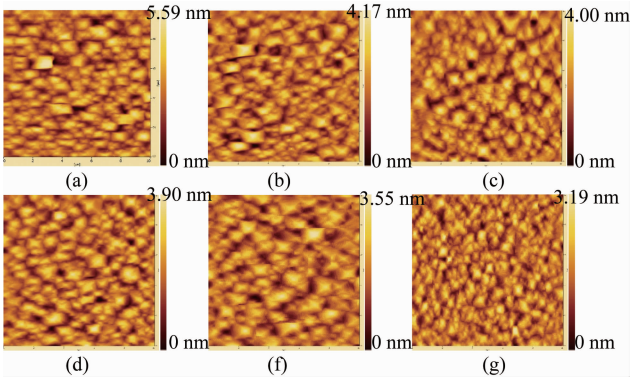

Fig. 3 AFM images of AlGaSb grown at various thickness. (a)100 nm, (b) 250 nm, (c) 500 nm, (d) 750 nm, (e) 1 μm, and (f) 1.5 μm
图 3 不同厚度的 AlGaSb 缓冲层原子力显微镜测试图片 (a)100 nm, (b) 250 nm, (c) 500 nm, (d) 750 nm, (e) 1 μm, and (f) 1.5 μm

However, due to the conductivity of AlGaSb is relatively higher than AlSb, thick AlGaSb buffer layer will cause current leakage problem. As shown in Fig. 5, with the increasing thickness of AlGaSb buffer, I_{off} of InAs/AlSb HEMT increases. Considering the current leakage problem caused by thick AlGaSb buffer layer, the proper thickness of the AlGaSb buffer layer is determined to be 250 nm.

2.2 Interface thickness between AlSb and InAs

As shown in Fig. 6, AlSb/InAs/AlSb structure was grown. InAs capper layer was deposited on AlSb barrier

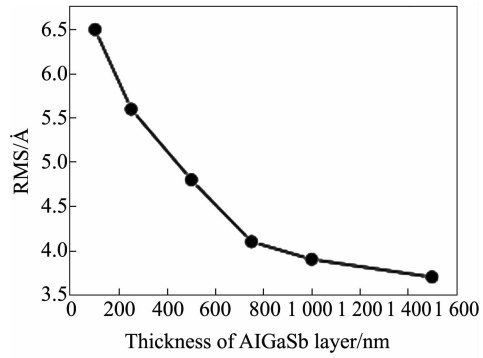

Fig. 4　AFM measurement value versus AlGaSb buffer thickness
图 4　不同厚度 AlGaSb 缓冲层的原子力显微镜测试结果

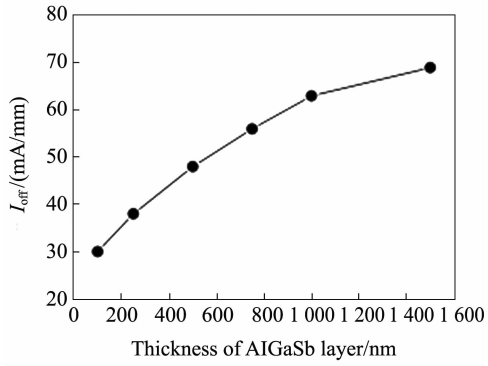

Fig. 5　I_{off} versus AlGaSb buffer thickness
图 5　不同厚度的 AlGaSb 缓冲层器件的关断电流测试结果

to prevent oxidation. In AlSb/InAs/AlSb sandwich structure, there is no common cation or anion between AlSb and InAs. And electron mobility of the sandwich structure with InSb-like interfaces is higher than the structure with AlAs-like interfaces[21-22]. The InSb-like interface is adopted in this structure, and the shutter sequence is shown in Fig. 7. Since the thickness of interface can also affect electron mobility, samples (a-d) were grown at different interface thickness (2 nm, 3 nm, 4 nm, and 5 nm).

Van der Pauw measurement results of samples (a-d) are shown in Fig. 8. From Fig. 8, electron mobility gradually decreases from sample (a) to sample (d) with the increased thickness of interface layer. In this work, 2 nm InSb interface is the proper thickness which can cause the decrease of electron density near the interface. The decrease of the electron density near interface can reduce the interface scattering. This makes high electron mobility in InAs channel.

2.3　Thickness of AlSb spacer

Since the thickness of AlSb spacer has influence on electron density and electron mobility in InAs channel, InAs/AlSb 2DEG structure samples (a-d) were grown with 3 nm, 5 nm, 7 nm, and 9 nm AlSb thickness. With a 5 nm AlSb spacer, the typical electron mobility of InAs/AlSb 2DEG structure is 20500 $cm^2/V \cdot s$, and the

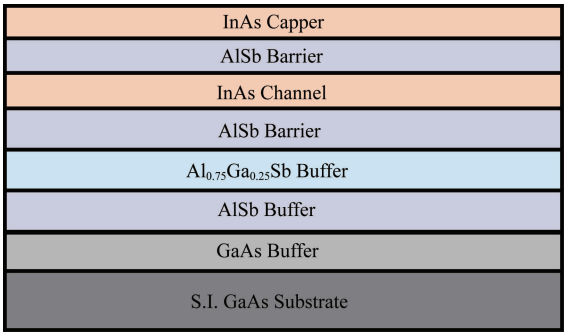

Fig. 6　Schematic diagram of AlSb/InAs/AlSb sandwich structure
图 6　AlSb/InAs/AlSb 三明治结构示意图

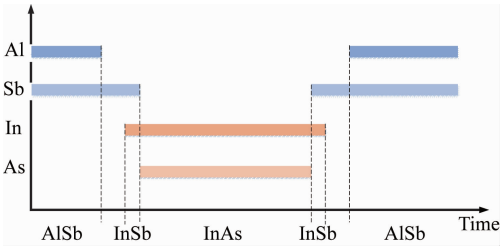

Fig. 7　Shutter sequence used to grow InSb-like interface
图 7　InSb 界面的快门顺序

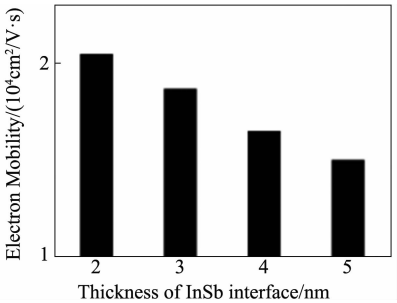

Fig. 8　Electron mobility versus InSb interface thickness (a)2 nm, (b) 3 nm, (c) 4 nm and (d) 5 nm
图 8　不同厚度 InSb 界面的电子迁移率测试结果 (a)2 nm, (b) 3 nm, (c) 4 nm, and (d) 5 nm

sheet electron density is in the range of $(2.0 \pm 0.3) \times 10^{12}/cm^2$.

As shown in Fig. 9, electron sheet density decreases with the increasing AlSb spacer thickness. Electron mobility increases from 3 nm to 5 nm AlSb spacer, then decreases from 5 nm to 9 nm AlSb spacer. When the spacer thickness increases from 3 nm to 5 nm, fewer electrons transfer to InAs channel from Si doping layer. Therefore, the ionization impurity scattering is reduced, and electron mobility increases. And with the increasing thickness of AlSb spacer, the confinement ability of quantum well weakens, which results in a decrease of the electron mobility[23].

3　Conclusions

$Al_{0.75}Ga_{0.25}Sb$ is designed as a buffer layer to ac-

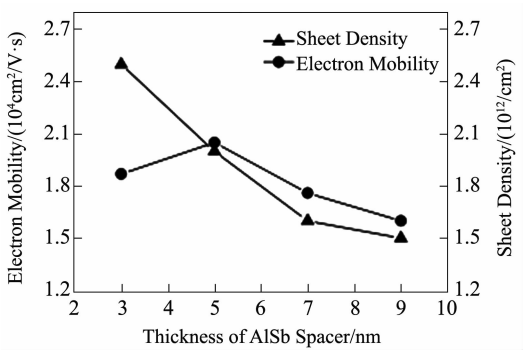

Fig. 9 Electron mobility and sheet density versus thickness of AlSb spacer. (a) 3 nm, (b) 5 nm, (c) 7 nm, and (d) 9 nm
图9 不同厚度 AlSb 隔离层的霍尔测试结果 (a) 3 nm, (b) 5 nm, (c) 7 nm and (d) 9 nm

commodate the large lattice mismatch between AlSb/InAs/AlSb sandwich structure and the S. I. GaAs substrate. The proper thickness of $Al_{0.75}Ga_{0.25}Sb$ buffer layer is determined to be 250 nm leading to improved surface morphology and less leakage current. Due to interface layer thickness between AlSb and InAs has an effect on electron mobility, the thickness of InSb was investigated and the optimum thickness of InSb interface layer is 2 nm. The proper thickness of AlSb spacer is about 5 nm. And the electron mobility of InAs/AlSb 2DEG structure is 20 500 $cm^2/V \cdot s$ with a sheet electron density of $2.0 \times 10^{12}/cm^2$. High-quality InAs/AlSb 2DEG structures were grown in this study and this type of device has potential application in high-speed and low-power integrated circuit design.

References

[1] Nguyen L D, Larson L E, Mishra U K. Ultra-high-speed modulation-doped field-effect transistors: A -torial review [J]. *Proceedings of the IEEE*, 1992, **80**(4): 494 - 518.

[2] Dingle R, Störmer H L, Gossard A C, *et al*. Electron mobilities in modulationdoped semiconductor heterojunction superlattices [J]. *Applied Physics Letters*, 1978, **33**(7): 665 - 667.

[3] Wang J, Wang G W, Xu Y Q, *et al*. Molecular beam epitaxy growth of high electron mobility InAs/AlSb deep quantum well structure [J]. *Journal of Applied Physics*, 2013, **114**(1):013704.

[4] Moschetti G, Zhao H, Nilsson P-Å, *et al*. Anisotropic transport properties in InAs/AlSb heterostructures [J]. *Applied Physics Letters*, 2010, **97**(24): 243510.

[5] Sasa S, Yamamoto Y, Izumiya S, *et al*. Increased electron concentration in InAs/AlGaSb heterostructures using a Si planar doped ultrathin InAs quantum well [J]. *Japanese Journal of Applied Physics*, 1997, **36**(1):1869 - 1871.

[6] Bennett B R, Ancona M G, Champlain J G, *et al*. Demonstration of high-mobility electron and hole transport in a single InGaSb well for complementary circuits [J]. *Journal of Crystal Growth*, 2009, **312**(1):37 - 40.

[7] Lin C, Chou Y, Lange M, *et al*. 0.1 μm n^+-InAs-AlSbInAs HEMT MMIC technology for phased-array applications: Compound semiconductor integrated circuit symposium, 2007 [C]. Portland, OR, USA: IEEE, 2007: 1 - 4.

[8] Ahmed I, Chowdhury S, Alam Md H, *et al*. Performance analysis of InAs/AlSb MOS-HEMT by self-consistent capacitance-voltage characterization and direct tunneling gate leakage current [J]. *ECS Transactions*, 2016, **72**(2):189 - 195.

[9] Tamilselvi S, Tamilarasi S, Mohanbabu A, *et al*. Analysis of noise performance in InAs DG-MOSHEMT: Devices for integrated circuit, 2017 [C]. Kalyani, India: IEEE, 2017:695 - 698.

[10] Guan H, Guo H. An optimized fitting function with least square approximation in InAs/AlSb HFET small-signal model for characterizing the frequency dependency of impact ionization effect [J]. *Chinese Physics B*, 2017, **26**(5): 058501.

[11] Bennett B R, Moore W J, Yang M J, *et al*. Transport properties of Be- and Si-doped AlSb [J]. *Journal of Applied Physics*, 2000, **87**(11): 7876 - 7879.

[12] Brar B, Leonard D. Spiral growth of GaSb on (001) GaAs using molecular beam epitaxy [J]. *Applied Physics Letters*, 1995, **66**(4): 463 - 465.

[13] Ghalamestani S G, Bergb M, Dick K A, *et al*. High quality InAs and GaSb thin layers grown on Si (1 1 1) [J]. *Journal of Crystal Growth*, 2011, **332**(1):12 - 16.

[14] Akahane K, Yamamoto N, Gozu S-I, *et al*. Heteroepitaxial growth of GaSb on Si(0 0 1) substrates [J]. *Journal of Crystal Growth*, 2004, **264**(1): 21 - 25.

[15] Kim Y H, Lee J Y, Noh Y G, et al. Growth mode and structural characterization of GaSb on Si (001) substrate: A transmission electron microscopy study [J]. *Applied Physics Letters*, 2006, **88**(24): 241907.

[16] Brar B, Leonard D. Spiral growth of GaSb on (001) GaAs using molecular beam epitaxy [J]. *Applied Physics Letters*, 1998, **66**(24): 463 - 465.

[17] Choi C H, Hultman L, Barnett S A. Ion-irradiation-induced suppression of three-dimensional island formation during InAs growth on Si (100) [J]. *Journal of Vacuum Science & Technology A*, 1990, **8**(3): 1587 - 1592.

[18] Zhao Z M, Hulko O, Yoon T S, *et al*. Initial stage of InAs growth on Si (001) studied by high-resolution transmission electron microscopy [J]. *Journal of Applied Physics*, 2005, **98**(12): 123526.

[19] Mano T, Fujioka H, Ono K, *et al*. InAs nanocrystal growth on Si (100) [J]. *Applied Surface Science*, 1998, **130-132**: 760 - 764.

[20] Proessdorf A, Grosse F, Romanyuk O, *et al*. Interface engineering for improved growth of GaSb on Si (1 1 1) [J]. *Journal of Crystal Growth*, 2011, **323**(1): 401 - 404.

[21] Tuttle G, Kroemer H, English J H. Effects of interface layer sequencing on the transport properties of InAs/AlSb quantum wells: Evidence for antisite donors at the InAs/AlSb interface [J]. *Journal of Applied Physics*, 1990, **67**(6): 3032 - 3037.

[22] Bolognesi C R, Kroemer H, English J H. Well width dependence of electron transport in molecular-beam epitaxially grown InAs/AlSb quantum wells [J]. *Journal of Vacuum Science & Technology B*, 1992, **10**(2): 877 - 879.

[23] WANG Hong-Pei, WANG Guang-Long, YU Ying, *et al*. Properties of δ GaAs/Al_xGa_1-xAs 2DEG with embedded InAs quantum dots [J]. *Acta Physica Sinica*. (王红培, 王广龙, 喻颖, 等. 内嵌 InAs 量子点的 δ 掺杂 GaAs/$Al_xGa_{1-x}As$ 二维电子气特性分析. **物理学报**), 2013, **62**(20): 422 - 427.